The cardiac, respiratory and gastric rhythms independently modulate corticospinal excitability

Tahnée Engelen[1]*, Teresa Schuhmann[2], Alexander T. Sack[2], Catherine Tallon-Baudry[1]*

Corresponding authors*:

tahnee.engelen@yahoo.nl

catherine.tallon-baudry@ens.psl.eu

Affiliations:

1. Cognitive and Computational Neuroscience Laboratory (LNC2), INSERM U960, Department of Cognitive Studies, Ecole Normale Supérieure, PSL University, 29 rue d'Ulm, 75005 Paris, France
2. Section Brain Stimulation and Cognition, Department of Cognitive Neuroscience, Faculty of Psychology and Neuroscience, Maastricht University, P.O. Box 616, 6200 MD, Maastricht, The Netherlands

Keywords:

Interoception, visceral rhythms, brain-body interactions, corticospinal excitability

Abstract

Interoception refers to the sensing of the internal state of the body and encompasses various bodily axes. Yet many interoceptive signals display unique qualities. The heart, lungs, and stomach each have their distinct frequencies, afferent pathways, and respective functions. At the same time each of these organs has been demonstrated to interact with neural activity and behaviour. To what extent then should different organs be treated as separate modalities in interoception? We here aim to answer this question by assessing in human participants whether the phase of these visceral rhythms is coupled to the corticospinal excitability of the motor system, and whether this coupling happens in an organ-specific or organ-general manner. We combined continuous physiological recordings with single pulse Transcranial Magnetic Stimulation (TMS) to probe phase-amplitude coupling between the phase of the cardiac, respiratory, and gastric rhythm and the amplitude of Motor Evoked Potentials (MEP). All three visceral rhythms contributed to MEP amplitude with similar effect sizes at the group level. However, we found no relation between coupling strengths with corticospinal excitability between the three organs. Thus, participants displaying high coupling with one organ did not necessarily display high coupling to the other organs, suggestive of unique interoceptive profiles. There was also no link between self-reported awareness of the organ and the actual

coupling, suggesting these are distinct dimensions of interoception. Together these results show that each coupling is mediated by at least partially independent mechanisms.

1. Introduction

Interoception refers to the sensing of internal bodily signals (Khalsa et al., 2018). Signals from the heart, lungs and stomach are considered a core component of interoception, from its original definition by Sherrington to current views (Khalsa et al., 2018; Nord & Garfinkel, 2022). Interoception is also functionally related to motor behaviour: typically, in “rest and digest”, activity in the gastro-intestinal tract is high while skeletomotor activity is low, while in “fight and flight” both the cardio-respiratory and skeletomotor systems are engaged. This simple example shows that interoception cannot be considered as a homogenous ensemble.

Indeed, the cardiac, respiratory, and gastric rhythms might reflect distinct interoceptive modalities (for review, see Engelen, Solcà, et al., 2023): they have distinct frequencies (respectively, 1Hz, 0.2 Hz and 0.05Hz), distinct physiological functions, and are generated either within the organs for the heart and stomach or in the central nervous system for respiration. While all three rhythms can influence brain activity through cranial nerves and spino-thalamic pathways, there are also rhythm-specific pathways. Respiration affects mechano-receptors in the olfactory system (Grosmaitre et al., 2007) and the cardiac rhythm, through blood pulse, directly affects the mechanosensitive Piezo2 channels of neurons (Jammal Salameh et al., 2024). As typically coupling between the brain and organs is quantified using different methods depending on the organ (e.g. heartbeat evoked potentials in the cardiac domain (Park & Blanke, 2019) or phase-amplitude and phase-phase coupling in the respiratory and gastric domain (Kluger & Gross, 2021; Rebollo et al., 2018; Richter et al., 2017) and many studies only target one organ alongside the brain at once, the amount of organ-specificity at the neural level is mostly still unclear. Answering this question would help narrowing down the type of mechanisms involved, and contribute to refining the very notion of interoception, with implications ranging from modelling to inter-individual variability and clinical applications.

We focus on the links between cardiac, respiratory and gastric activity and motor system excitability (Figure 1), probed non-invasively by measuring Motor Evoked Potentials (MEPs) induced by Transcranial Magnetic Stimulation (TMS) over primary motor cortex in humans (Bestmann & Krakauer, 2015; Spampinato et al., 2023). MEPs typically measure excitability from primary motor cortex to the final muscle where they are measured, including spinal relays. Different lines of evidence suggest that motor excitability varies with the three visceral rhythms. Movement onsets (Galvez-Pol et al., 2020; Konttinen et al., 2003; Kunzendorf et al., 2019; Ohl et al., 2016; Palser et al., 2021), response inhibition (Rae et al., 2018), discharge of alpha motoneurons (Ford & Kirkwood, 2018), and MEP amplitude (Al et al., 2023) vary along the cardiac cycle. The phase of respiration affects the timing of voluntary (Johannknecht &

Kayser, 2022; Park et al., 2020) and involuntary (Schulz et al., 2016) actions, motor-related neural activity (cortical readiness potential (Park et al., 2020), beta coherence (Kluger & Gross, 2020), and changes in breathing style influence MEPs (Li & Rymer, 2011; Shirakawa et al., 2015). For the gastric rhythm, evidence is more scarce but this rhythm is consistently coupled to motor and premotor areas at rest in humans (Rebollo et al., 2018; Rebollo & Tallon-Baudry, 2022) as well as in anaesthetized rodents (Cao et al., 2019, 2022).

Here, we experimentally test whether interoception is organ-specific by examining if the phase of the three visceral rhythms is coupled to fluctuations in the amplitude of MEPs, and whether the coupling is similarly strong for each rhythm at the group level. We then analyze individual profiles to determine if intersubject variability suggests that interoceptive coupling with motor excitability is global, or organ-specific – in other words, do participants with strong cardiac-motor coupling also display high respiratory- and gastric-motor coupling, or are participants defined by specific coupling with one organ? Lastly, we examine whether the self-reported awareness of each of the organs was related to the strength of viscera-motor coupling.

2. Materials & Methods

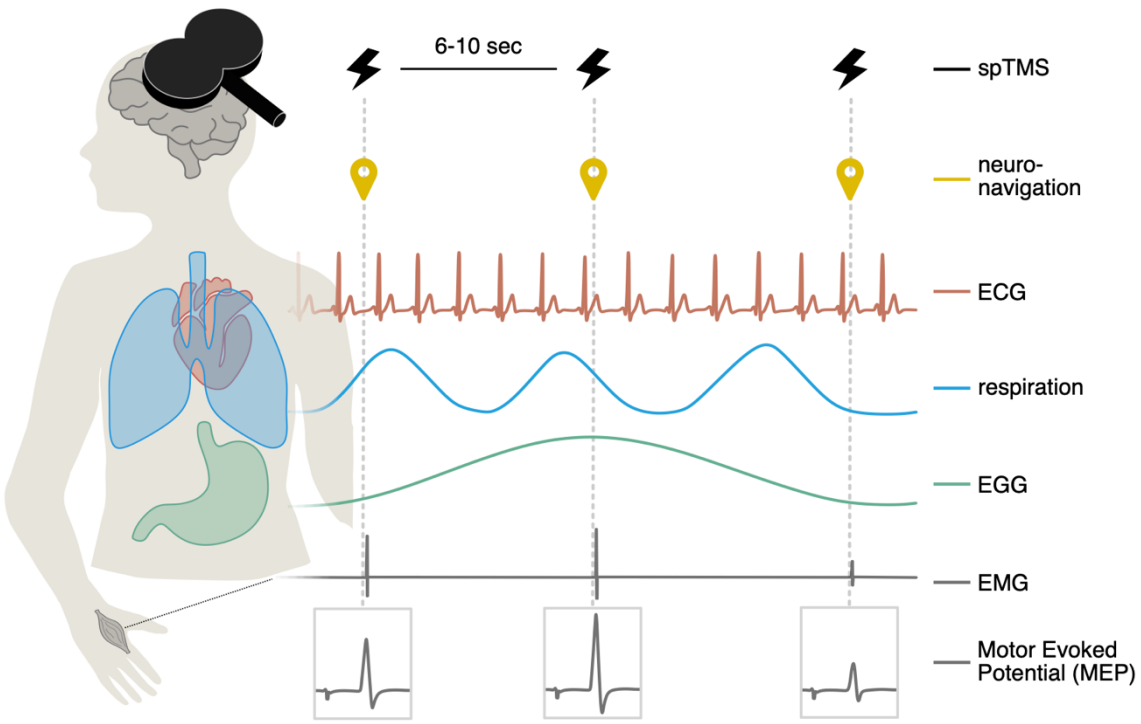

Figure 1. Experimental set up. Single pulses of TMS were applied to the hand area of the right primary motor cortex with an inter-pulse interval randomized between 6 and 10 seconds. Simultaneously, the neuronavigated coil position (yellow), electrocardiogram (red), respiratory signal (blue), electrogastrogram (green) and electromyography from the left hand (gray) were recorded. The experimental measure was the Motor Evoked Potential (MEP) amplitude measured on a hand muscle (first dorsal interosseous), analyzed against the phase of the cardiac, respiratory and gastric rhythms. Note that the three rhythms have very different periods (~1s for the heart, ~5 s for respiration, and ~20s for the gastric rhythm).

2.1 Participants

29 healthy participants completed the experiment after providing written informed consent. The study was approved by the Ethics Review Committee Psychology and Neuroscience of Maastricht University (reference number ERCPN-247_01_01_2022). Participants received a voucher reward of 10 euros per hour. Inclusion criteria were to be aged above 18 years and to have a Body Mass Index (BMI) smaller than 25 to ensure good quality gastric recordings. Participants were further screened for MRI and TMS safety. One participant was excluded from analysis due to issues with recording of the respiration signal. In total, 28 participants were included in the final analysis (8 male, 2 left handed, mean age(SD) = 27.36(8.98), mean BMI(SD) = 21.76(2.38)).

2.2 Experimental procedure, general organization

The experiment consisted of two sessions. During the first session an anatomical MRI scan was acquired at rest. At the start of the second session participants completed the questionnaires, after which all physiological recordings were prepared and TMS intensity and stimulation site were determined. Participants completed three blocks of the task, each lasting around 16 minutes, while the TMS stimulation was applied, during which they were in a seated position with their head supported by a chin rest. Participants were instructed to fixate on a screen and were given a task to avoid drowsiness (see 2.5).

2.3 TMS application and neuronavigation recordings

Single pulse TMS was applied over right M1 hotspot using a MC-B70 figure-of-eight coil and Magpro X100 stimulator (MagVenture A/S, Farum, Denmark). Participants were co-registered to their individual anatomical T1 MRI (TR = 2300 ms, TE = 2.98 ms, TI = 900 ms, 192 slices, FOV = 256 mm, matrix sixe = 256 × 256, 1 mm isotropic voxel, acquired on 3T Siemens Prisma Fit) and coil position was recorded throughout the session using a neuronavigation system (Localite GmbH, Bonn, Germany). The coil was placed tangentially to the scalp with the handle pointing backward at a 45-degree angle from the midline. Individual stimulation intensity was set to elicit an MEP of approximately 1mV in amplitude (mean stimulation intensity(SD) = 41(7)% maximum stimulator output). The stimulation target was identified by applying single pulses over the right hemisphere until the location showing a maximum response from the left first dorsal interosseous muscle (FDI) was found, which was set as the target for the rest of the session. The interpulse interval was jittered between six and ten seconds and a total of 360 pulses were applied during the task, subdivided into three blocks. The difference between coil and target location was calculated off-line as follows:

$$\text{Coil distance} = \sqrt{(dP^2 + dS^2 + dL^2)}$$

where *dP*, *dS*, and *dL* are the difference between location of the coil and the set target in the Posterior, Superior, and Lateral dimensions. Trials on which the coil distance exceeded more than four standard deviations from the mean of the participant were excluded from analysis.

2.4 Physiological recordings

Physiological signals were recorded using a BrainAmp ExG amplifier and the BrainVision Recorder software (Brain Products GmbH, Gilching, Germany) at a 5000Hz sampling rate. All signals were recorded with a high cut-off of 1000Hz and with a low cut-off filter set to a time constant of 10 seconds for electromyography (EMG) and the electrocardiogram (ECG) and

DC for respiration and the electrogastrogram (EGG). A respiration belt containing a pneumatic pressure-sensitive cushion was placed around the chest to record thoracic respiratory movements. All other signals were recorded with bipolar montage using cutaneous AgCl ring electrodes. Motor evoked responses were recorded using EMG of the left FDI muscle following the belly-tendon montage with one electrode placed over the belly of the muscle and a reference electrode placed along the outside of the index finger. The ECG was recorded by placing one electrode below the right clavicle and the other electrode on the left lower abdomen (lead II). The EGG was recorded using a grid of six electrodes on the left side of the belly, all referenced to an electrode on the upper right side of the belly, following recommendations of Wolpert et al. (2020).

2.5 Task and eyetracking

To help participants remaining wakeful during data acquisition, one quadrant of the black circle surrounding the fixation point could occasionally turn white for 500ms. In each block 16 targets were randomly presented, always starting/ending with at least 500ms distance to the TMS pulse. To avoid contamination of manual motor actions on MEP amplitude, participants responded by making an eye movement to the corner of the screen in the direction at which the target appeared. Eye position was tracked using an Eyelink 1000 system (SR Research, Canada), using a monocular recording of the right eye with a 16mm lens at a sampling rate of 1000 Hz.

2.6 Questionnaires

To measure self-reported interoception, participants completed two questionnaires prior to the start of the experiment, the Three-domain Interoceptive Sensations Questionnaire (THISQ) (Vlemincx et al., 2023) and the Multidimensional Assessment of Interoceptive Awareness, Version 2 (MAIA-2) (Mehling et al., 2018).

2.7 Data pre-processing

Offline pre-processing and analysis of physiological signals was done using the Fieldtrip toolbox implemented in Matlab (Oostenveld et al., 2011) and additional custom-built Matlab code.

Continuous EMG data was band-pass filtered between 1 and 1000Hz using a 4th order forward and backward Butterworth filter and segmented around the TMS pulse (-1 to +1 second). MEP amplitude was calculated as the difference between the local maximum and local minimum between 20-60ms after the pulse. MEPs were excluded if their amplitude was below 50μV,

their amplitude got cut off due to amplifier saturation, their amplitude exceeded the mean of the participant by more than four standard deviations, or if the signal to noise ratio (SNR) between the time preceding the pulse relative to the MEP amplitude was below three. SNR was calculated as the amplitude of the MEP divided by the maximum RMS value in the 500-10ms preceding the pulse.

Continuous ECG data was band-pass filtered between 1 and 40 Hz (windowed-sinc FIR filter, onepass-zero phase shift). A participant and block specific template heartbeat was computed and convolved with the ECG time series. R-peaks were identified on the normalized convolution as exceeding a threshold of 0.6. Misidentified R-peaks were manually corrected. Further cardiac events were defined relative to the R-peak as local minima or maxima in preset time windows. For the T-wave this was a local maximum occurring within 420ms after the Q-wave. Noisy cycles were identified by excluding any cycles in which the RT interval exceeded 3 standard deviations from the mean of that block. Instantaneous cardiac phase was calculated by assigning radian values between 0 and 2π to each TMS pulse based on its relative timing within the RR interval. To further characterize systole and diastole, we determined the end of the T-wave. A block-by-block mean T wave was computed, and the local maximum in the second derivative of this signal in between the peak of T up to + 150ms was found. The mean end of T time between the three blocks was used to define cardiac systole (R peak to end of T) and cardiac diastole (end of T to next R).

Continuous respiration data was smoothed using a 750ms window moving average (Matlab movmean). Expiration onset was identified on the z-scored respiration signal using the findpeaks function with a minimum peak distance of 1 seconds and minimum peak prominence set to the mean positive peak height excluding extreme values (peaks exceeding three times the standard deviations from the mean signal are excluded). The beginning of inspiration was determined by using an adapted version of the trapezoid area algorithm (Vázquez-Seisdedos et al., 2011). Briefly, this involved iteratively fitting trapeziums on the derivative of the respiration signal, and finding the area where the trapezoid has the largest area, which is taken as inspiration onset. Artefacted segments were identified by manual inspection. Cycles with either inspiration or expiration length exceeding the mean length of inspiration and expiration of the respective block by four SDs were excluded from further analysis. Instantaneous respiratory phase was calculated by assigning radian values between 0 and 2π to each TMS pulse based on its relative timing to the start of inspiration and end of expiration interval.

EGG data was preprocessed following the steps described in Wolpert et al. (2020). Data was demeaned, detrended, and down-sampled to 1000Hz. A Fast-Fourier Transform (FFT) with a Hanning taper was used to identify the channel with the largest spectral activity in the normogastric range (0.033-0.067Hz), which was then selected for further analysis. Data was band-width filtered around individual peak frequency ±0.015Hz using a third-order finite impulse responses filter (Matlab FIR2). Artefacted segments were identified as cycles whose length exceeded three SDs from the mean cycle length (except two participants where SD criterion of two was used due to noisier data) or which displayed nonmonotonic changes in phase. Instantaneous phase was retrieved by Hilbert transforming the filtered data.

After preprocessing, a mean(SD) of 287(41) out of 360 trials remained for analysis (min: 191 ; max: 342).

2.8 Statistical analysis

2.8.1 General

General support for or against the null hypothesis was quantified using the Bayes Factor (BF) using formulas provided by Liang et al. (2008). BF_{10} values smaller than 0.33 indicate moderate support for H_0, and values smaller than 0.1 indicate strong evidence for H_0. On the other end, values exceeding 3 indicate support for H_1, and values exceeding 10 indicate strong evidence for H_1. Reported effect sizes are quantified using Hedge's g (Matlab meanEffectSize), where effects above 0.2 are considered small, 0.5 considered medium, and 0.8 considered large. Reported correlations are calculated based on Kendall's tau B implemented in JASP (JASP Team (2024)) and a False Discovery Rate (FDR) correction of p-values is applied if necessary.

2.8.2 The effect of coil distance on MEP amplitude

To account for the effect of displacement of the TMS coil with respect to the participant's head, we modeled the influence of coil distance on the MEP amplitude. This is particularly relevant given that head displacement caused by the participant's respiratory rhythm could potentially explain phase locked amplitude changes. We modelled the trial-by-trial z-scored peak to peak amplitude of the MEP with the z-scored coil distance value for each participant separately using a general linear model (GLM) in the following manner:

$$[z(MEP_{amplitude})] \sim \beta_0 + \beta_{coil\ distance} * [z(\text{Coil distance})] + MEP_{residuals}$$

To test for significance, the beta values for the coil distance regressor were tested against zero using a two-tailed paired t-test. Given the significant result of this analysis, all subsequently described analyses are performed on the residuals resulting from this model. In other words, our analyses of interest are performed on amplitude values which have been corrected for the effect of coil distance.

2.8.3 Assessing phase-amplitude coupling between visceral rhythms and MEPs

To test whether the amplitude of the MEP was coupled to the phase of either the cardiac, respiratory, or gastric rhythm (visceral phase with MEP amplitude coupling), we used a circular spline generalized circular model (Kramer & Eden, 2013). This method allows for assessing phase-amplitude coupling that is either mono- or biphasic (Hülsemann et al., 2019), and by computing participant specific chance level does not require phase-alignment on the group level, which is unlikely to be the case for the gastric rhythm where there is no true zero point in the cycle (Wolpert et al., 2020). Importantly, this analysis thus tests whether there is higher phase-amplitude coupling than chance level. Briefly, the circular GLM (normal distribution, identity link function) involves fitting two models, the spline model in which cardinal splines are fitted to each participant's data to estimate amplitude as a function of phase, and a null model. The spline model is fitted based on a number of control points which is estimated for each participant separately using the Akaike information criterion (mean(SD) control points for cardiac = 4.5(1.4), for respiration = 4.7(1.3), and gastric = 4.7(1.6)). In the null model each data point corresponds to the mean of the data, generating data with a uniform distribution along phase. To quantify phase-amplitude coupling the maximum absolute deviation between the spline and null model is calculated (r value). The larger the r value, the more the empirical data deviate from a uniform distribution. We ran one model *per visceral signal* (thus three models) and *per participant* to obtain individual empirical r values.

Importantly, large r-values could be obtained by chance. Thus, to further determine whether the significance of empirically obtained r values, we estimated the chance distribution of r values for each participant. We ran the model described above 1000 times, each time shuffling the phase labels associated to each trial. A participant's coupling strength was then computed by subtracting the median of the permuted r value distribution from the empirical r value. Because circular spline GLMs allow for only one circular regressor, we thus tested each visceral rhythm separately. Statistical significance of coupling strengths at the group level was assessed with a one-sided t-test against zero.

Lastly, we wanted to test for the inter- or independence of coupling of the different visceral rhythms to the motor system in another manner besides correlations between the coupling

strengths, to ensure our findings are not simply a result of our chosen analysis technique. To this end we opted for a simple GLM, similar to the one used to estimate the effect of coil distance on MEP amplitude, in which all three visceral rhythms are entered as well as their interactions. To be able to analyse circular data, such as visceral phase, in a simple GLM required the binarization of the data. To this end, the visceral phases were split into one 'excitatory' and one 'inhibitory' phase based on each individual's data. For each participant, data was divided into six equally spaced phase bins between 0 and 2pi. Excitatory phase was defined as the phase bin with the highest mean residual MEP values and the two adjacent bins, and inhibitory phase consisted of the three remaining bins.

This approach allowed us to add all three visceral rhythms and their interactions into the same model (rather than one model per signal), which was not possible in the circular spline model. The influence of binary visceral phase on the residual values was then estimated in the following way:

$$MEP_{residuals} \sim \beta_0 + \beta_{cardiac\ phase} + \beta_{respiratory\ phase} + \beta_{gastric\ phase} + \beta_{cardiac\ *\ respiratory\ phase} + \beta_{respiratory\ *\ gastric\ phase} + \beta_{cardiac\ *\ gastric\ phase} + \beta_{cardiac\ *\ respiratory\ *\ gastric\ phase}$$

Importantly, this model did not aim to see if the phase of each visceral rhythm explains the MEP residuals, as this was already established with the spline models, and phase effects are here enforced by splitting the data based on optimal phase. Rather, the goal was to be able to investigate the interaction effects on the MEP residuals, as these speak to whether the visceral phase effects previously observed are independent. To test for significance of the interaction terms, the beta values of the interaction term regressors were tested against zero using a two-tailed paired t-test.

2.8.4 The relationship between viscera-motor coupling and self-reported interoception

We wanted to test for any relationship between objective measures of brain-viscera coupling and the extent to which participants themselves indicate to be aware of their internal organs. To do so, we correlated each participants organ-specific coupling strength with the matching organ specific scores obtained in the THISQ questionnaire (e.g. cardiac coupling strength correlated with cardiac THISQ score). We also tested for a correlation between coupling strengths and a widely adopted interoception questionnaire, the MAIA-2 (Mehling et al., 2018). For the correlation analysis we focused on the correlations between the coupling strengths and the body listening and noticing sub-scores, which refer to the awareness of bodily signals and active listening to the body for insight respectively, as they were closest to our research

questions. Correlations with the MAIA questionnaires were FDR corrected for six tests (two sub-scores by three coupling strengths).

2.8.5 Inter-individual variability in the alignment to physiological phases

The circular spline GLM specifically tests whether there is phase-amplitude coupling between the visceral rhythms and corticospinal excitability, however it does not conclude anything about whether the exact optimal phase is consistent between participants. This means that one participant could have a strong increase in excitability early in the cardiac phase and another late in the cardiac phase. However, based on existing literature such increases in motor excitability might occur in specific moments in either the cardiac or respiratory cycle (e.g. Al et al., 2023; Park et al., 2020). To explore this possibility, for each participant we divided the data into six equally spaced phase bins between zero and 2pi, and extracted their mean bin residual value, and which bin had the highest mean. We here specifically focused on the data wrapped to the physiologically meaningful phases, so bins between zero and pi represent either systole or inspiration, and between pi and 2pi represent either diastole or expiration. This analysis allows looking at whether group mean bin values show patterns across the cycle, and whether the highest bin is consistent on the group level.

Note that here we do not further examine the gastric rhythm, as the exact starting point of each cycle is unknown and thus looking at group level consistency is not meaningful.

3. Results

3.1 Coil distance-to-target explains MEP amplitude

The distance of the TMS coil to the target in the motor cortex is likely to influence MEP amplitude. This distance varies with experimenter and/or participant movement and might thus be related to the participant's breathing movement, which would confound all further analysis. Our first step was thus to explain MEP amplitude with coil distance-to-target, using a GLM. Smaller distance of the coil to the target resulted in larger MEP amplitudes (paired -t-test against 0, $t(27) = -5.26$, $p < 0.001$), with a BF_{10} of 1475 indicating strong support for the alternative hypothesis, and a Hedge's g of -0.97 indicating a large effect (see figure 2A). To control for the extent to which fluctuations in coil distance-to-target explain MEP variability, all subsequently reported analyses are performed on the MEP residuals of this model, i.e., fluctuations in MEP amplitude not explained by fluctuations in coil distance-to-target.

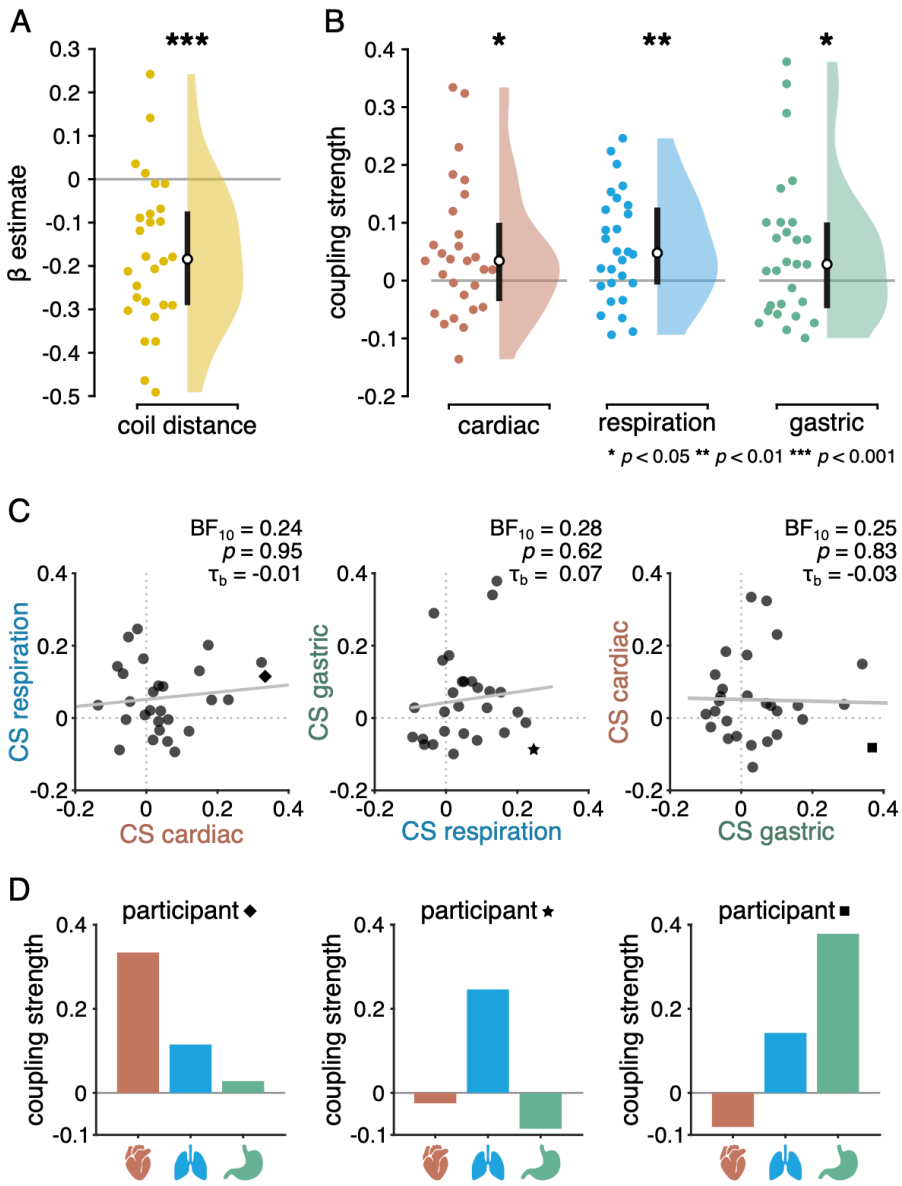

Figure 2. A) Modeling fluctuations in MEP amplitude with the distance of the coil to the target showed that larger distances result in significantly smaller MEPs. In all subsequent analyses, the influence of coil-to-target distance is regressed out from MEP amplitude. B) Coupling strengths (CS) between each visceral rhythm and MEPs. CS reflects the difference between empirical and chance level coupling estimated with a circular GLM. Coupling strengths were significantly larger than zero for the cardiac, respiratory, and gastric rhythm. This means that the phase of the visceral rhythms impacted the amplitude of the MEP C) The phase-amplitude coupling between the viscera and motor cortex happened independent from one another, there were no significant correlations between the coupling strengths of the different organs. D) Interoceptive profile of the participant with the largest cardiac-motor coupling (left, lozenge in C), the largest respiration-motor coupling (middle, star in C), and the participant with the largest gastric-motor coupling (right, square in C). High coupling between corticospinal excitability and a given organ did not imply high coupling between corticospinal excitability and the two other organs investigated. Each participant displayed a unique interoceptive profile. * $p<0.05$; ** $p<0.01$; *** $p<0.001$

3.2 The amplitude of MEP is coupled to the phases of the three visceral rhythms

We first wanted to establish whether, as hypothesized, there was coupling between the phase of each of the visceral rhythms and the amplitude of the MEP. Phases are defined from R peak to R peak for the cardiac rhythm, from beginning of inspiration to end of expiration for the respiratory rhythm, and are unrelated to specific physiological events for the gastric rhythm, where such markers do not exist (Wolpert et al., 2020).

Using a circular spline GLM approach (Kramer & Eden, 2013), we estimate, for each participant, how much MEP amplitude varies with the phase of each visceral rhythm. We compute coupling strengths, reflecting the difference between empirically obtained coupling scores and the median of chance level coupling scores obtained by permutation. We found coupling strengths to be significantly larger than zero for the cardiac (t-test against 0, $t(27) = 2.29$, $p = 0.015$, $BF_{10} = 3.65$, Hedge's g = 0.54), respiratory ($t(27) = 3.21$ $p = 0.002$, $BF_{10} = 22.91$, Hedge's g = 0.54), and gastric ($t(27) = 2.15$, $p = 0.02$, $BF_{10} = 2.85$, Hedge's g = 0.49) rhythms (see figure 2B). This result demonstrates that fluctuations of corticospinal excitability over time are partially driven by the phase of each of the three visceral rhythms with similar effect sizes.

3.3 Cardiac, respiratory, and gastric phase influence corticospinal excitability independently

Given known interactions between the visceral rhythms (e.g. cardiac-respiratory coupling) and the existence of shared anatomical pathways (e.g., vagus nerve), we wanted to test whether the visceral phase effects on corticospinal excitability were related to, or independent from, one another. We first tested for this possibility by correlating the individual coupling strengths of the three visceral rhythms with corticospinal excitability with each other. We found no correlation between coupling strength with motor cortex of the three different visceral rhythms, with all tested correlations providing moderate evidence for the null hypothesis (Kendall's tau

B correlations, all p values > 0.62, all BF_{10} < 0.33, see figure 2C). By exploring the interoceptive profiles of the participants with the highest coupling strength of each rhythm, it is apparent that high coupling with one rhythm does not necessarily mean high (or any) coupling with another rhythm, and all types of interoceptive coupling profiles can be possible, as illustrated in figure 2D.

We confirmed those results using a second approach, where all rhythms were combined in the same general linear model. To switch from a circular spline model to a general linear model with interactions between rhythms, we defined for each participant and each rhythm an interval of pi where MEP amplitude was maximal (excitatory phase), and an interval of pi where MEP amplitude was minimal (inhibitory phase). For each participant, we then accounted for MEP amplitude by binarized phases for all three rhythms, and, importantly, all possible interactions between rhythms. The model confirms a significant influence of all three rhythms, as expected by the model design, but revealed an absence of interactions between rhythms: We found no double or triple interactions between any of the visceral phases (all p values for interaction terms > 0.18). Except for the interaction term between cardiac and gastric phases (BF_{10} = 0.47), all BF_{10} values indicate moderate evidence for the null for all other interactions (BF_{10} < 0.33).

These separate analyses show that even though the phase of each of the three visceral rhythms influences the amplitude of the MEP, they do so in an independent manner.

3.4 No link between self-reported interoception and viscera-motor coupling

We wanted to assess whether the strength of an individual's coupling between visceral phase and corticospinal excitability, was related to how much an individual indicates to be aware of this specific organ. To this end, we correlated the coupling strength of each of the organs to the organ specific scores of the recently developed THISQ questionnaire (Vlemincx et al., 2023). There was no significant correlation between these two interoceptive measures (Kendall's tau B correlations; all p > 0.10) and BF_{10} values indicate moderate evidence for the null for the gastric data (BF_{10} = 0.25) and an undecided Bayes Factor for the cardiac and respiration data (BF_{10} = 0.93 and BF_{10} = 0.47 respectively, see figure 3). This suggests whether a participant has high subjective awareness of their heart, lungs, or stomach, is unrelated to the extent to which the organ's rhythm is coupled to motor cortex excitability.

Additionally, we tested whether viscera-motor coupling strengths were linked to a commonly used interoception questionnaire (MAIA-2 (Mehling et al., 2018)) that mixes different organs

into the same score or sub-score. We specifically focused on the sub-scores most related to awareness of internal sensations, body listening and noticing. Again, we find no significant correlations with either body listening (cardio p_{FDR} = 0.30, τ_b = 0.21, BF_{10} = 0.75, respiration p_{FDR} = 0.29, τ_b = -0.27, BF_{10} = 1.74, gastric p_{FDR} = 0.89, τ_b = -0.02, BF_{10} = 0.25), or noticing (cardio p_{FDR} = 0.66, τ_b = -0.08, BF_{10} = 0.29, respiration p_{FDR} = 0.3, τ_b = -0.20, BF_{10} = 0.71, gastric p_{FDR} = 0.35, τ_b = -0.167, BF_{10} = 0.51).

Together these results show that different questionnaires measuring the extent to which someone feels aware of their body (either organ-specific or more generally speaking) is unrelated to the extent to which there is motor-viscera coupling, highlighting how these measures tap into different dimensions of interoception.

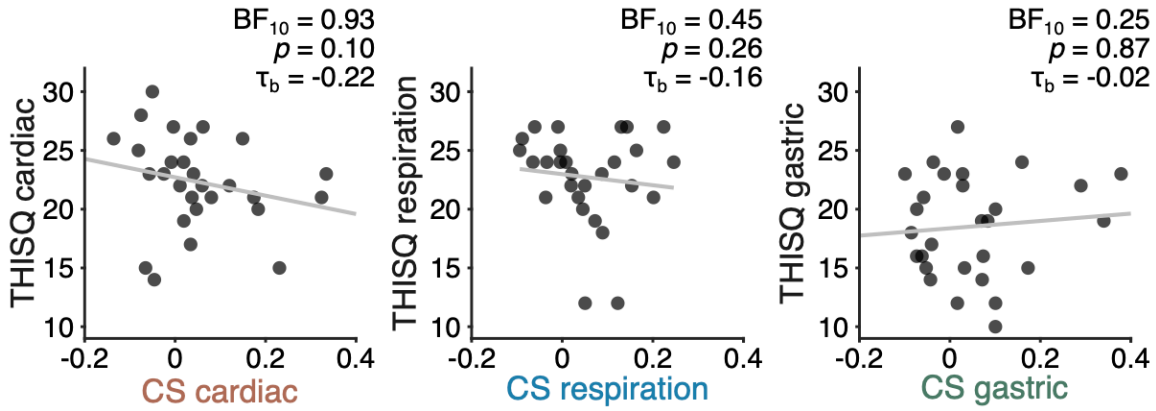

Figure 3. No correlation between self-reported organ-specific interoception on the THISQ questionnaire and the respective coupling strength (CS) with corticospinal excitability of that organ.

3.5 Alignment to cardiac and respiratory phase shows inter-individual variability

The cardiac and respiratory rhythms can be subdivided in two meaningful physiological phases, respectively systole/diastole and inspiration/expiration. As an exploratory analysis we tested whether the observed modulation of excitability along the cardiac and respiratory cycle is aligned with those physiological phases, and assessed the extent of inter-individual variability in this alignment.

In line with previous findings (Al et al., 2023), at the group level, corticospinal excitability was enhanced in the systolic cardiac phase (figure 4A, left). In terms of variability, 20 out of 28 participants had their highest phase bin in the systolic phase (figure 4A, right), showing that most, but not all, participants followed the pattern for cardiac enhancement during systole. Regarding respiration, at the group level, corticospinal excitability was largest in early inspiration (figure 4B, left). This pattern is consistent with previously reported increased amplitudes of the readiness potential during inspiration (Park et al., 2020), although the same

study reported more action onsets during the end of expiration, potentially showing how different stages of motor output can be impacted by visceral phase. However, inter-subject variability appeared a bit larger than for cardiac phase: 17 out of 28 participants had their maximal MEP amplitude during inspiration (figure 4B, right).

While group data suggest preferential phases of enhanced excitability, during cardiac systole and at the beginning of inspiration, there was also large inter-subject variability. We therefore further tested whether participants who deviated from the group pattern for cardiac phase also deviated from the group pattern for respiratory phase. As illustrated in Figure 4C, some participants followed the group pattern for both systole and inspiration (participant 8), others showed systolic coupling, but late expiration coupling (participant 7), some showed no coupling to the cardiac cycle, but an increase during inspiration (participant 22), and lastly an example showing coupling to both of the rhythms, yet both divergent from the group pattern (participant 26).

This exploratory analysis reveals that although group level effects might indicate alignment to physiological phases of the cardiac and respiratory rhythms, some participants deviate from this alignment yet still display robust coupling with the corticospinal excitability.

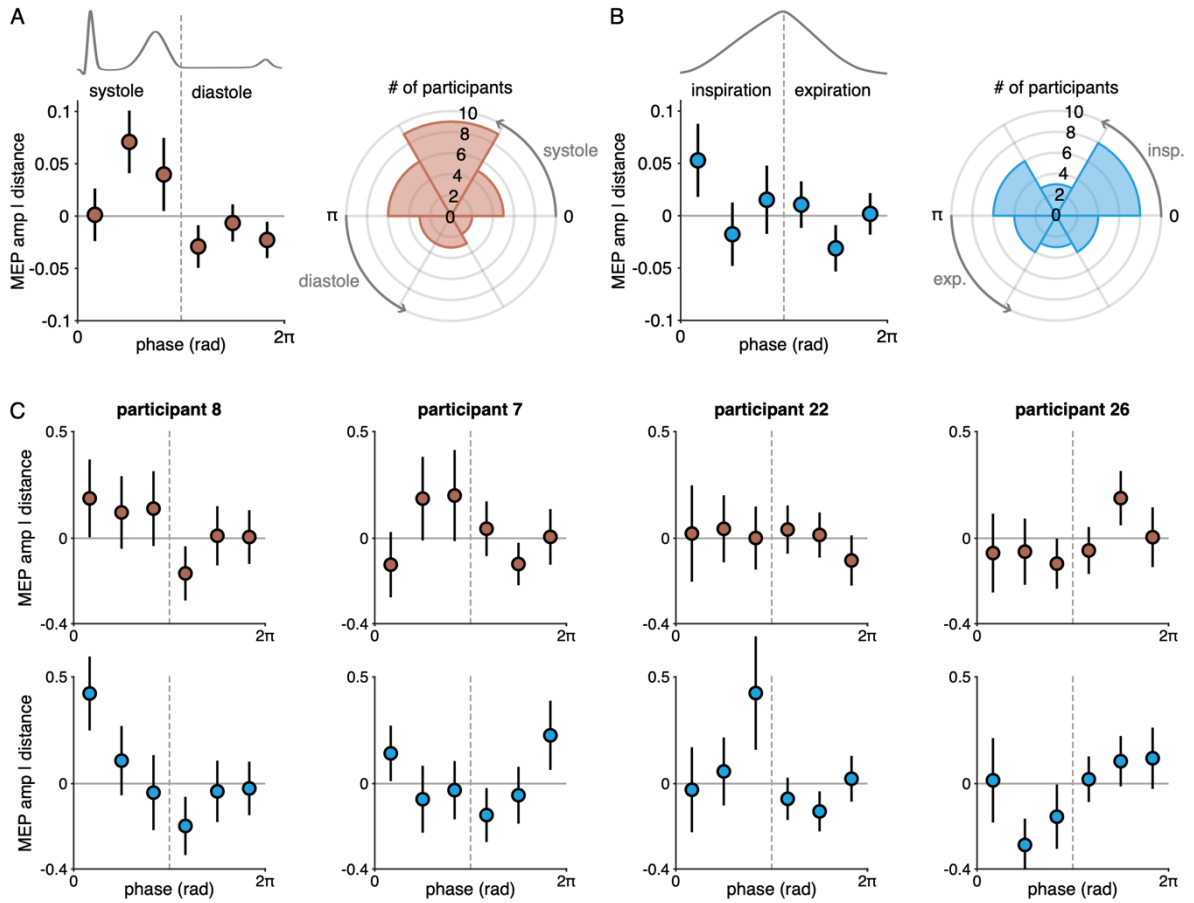

Figure 4. Exploratory analyses on alignment to physiological phases for the cardiac and respiratory rhythm. A) Phase-binned mean MEP amplitudes showed greatest enhancement in the systolic cardiac phase (left), with 20/28 participants having their highest bin mean during systole (right). B) Phase-binned mean MEP amplitudes showed greatest enhancement in the early inspiration phase (left), with 17/28 participants having their highest bin mean during inspiration (right). C) Examples of individual data. Though overall patterns locked to physiological phases emerge on the group level, participants can still display individual coupling patterns of MEP enhancement along the cardiac or respiratory phase.

4. Discussion

To quantify organ-specificity in the coupling between interoception and the motor system, we tested whether the phase of the cardiac, respiratory, and gastric rhythm can explain fluctuations in corticospinal motor excitability. We quantified individual levels of organ-motor coupling from the same brain region using the exact same outcome measure in a within-participant design, thereby making such direct comparisons more meaningful. We were able to demonstrate, for the first time, that coupling between the corticospinal tract and the cardiac, respiratory, and gastric rhythm have similar effect sizes at the group level, and within the same participant can happen independently from one another. Participants displayed their own individual interoceptive profiles, where any combinations of high/low viscera-motor coupling were possible. Furthermore, we found levels of viscera-motor coupling to be unrelated to participant's self-reported awareness of these organs, suggesting these measures tap into distinct interoceptive dimensions. Altogether, our results suggest that the coupling between the motor system and each visceral organ is mediated by distinct mechanisms.

4.1 Viscera-motor coupling is robust

Post-hoc power analysis showed that given our effect size we had >80% power (Faul et al., 2007), meaning our sample was sufficiently large to robustly demonstrate the effect of visceral phase on MEP amplitude. Our effects cannot be explained by movements induced by the physiological rhythms as we controlled for the distance between the coil and our stimulation target, which similarly to previous work significantly explained MEP variability (Claudino et al., 2018). Although some previous work showed effects of cardiac phase on MEP amplitudes (Al et al., 2023), there have also been reported null findings (Bianchini et al., 2021; Filippi et al., 2000; Otsuru et al., 2020; Paci et al., 2024). This discrepancy is likely explained by differences in the experimental design, such as TMS locking to fixed cardiac phases, which might miss the inter-individual variability in optimal phases demonstrated in this experiment, as well as variance in coil to target, which was not taken into account in those studies.

4.2 Distinct organ-specific mechanisms mediate viscera-motor coupling

Our results show that corticospinal excitability is independently related to the cardiac, respiratory and gastric rhythms. Those independent links have similar effect sizes, but reflect a large inter-individual variability, with idiosyncratic profiles of interoceptive-motor coupling. Those two findings - independence between the different coupling types and the existence of idiosyncratic profiles - suggest that each coupling is mediated by distinct mechanisms. There are various candidates for how the three rhythms might independently impact the motor system: unique afferent pathways, separate target sites in the motor system, potentially

involving different neurotransmitters and neuromodulators, or effects at the spinal or peripheral levels.

Independent influences of rhythmic organ activity on motor cortex excitability might be the result of unique afferent pathways. While all three organs are connected to the central nervous systems through cranial nerves and spino-thalamic pathways, there are also specificities. For instance, cardiac inputs translate into changes in blood pressure, that can be transduced directly by neurons and glial cells (Jammal Salameh et al., 2024; Kim et al., 2016). Nasal respiration is transduced in the olfactory bulb and induces neural oscillations in large cortical territories (Gonzalez et al., 2023; González et al., 2023; Tort et al., 2010; Zhuang et al., 2019).

The cortical motor areas control visceral organs, including separate representations of the stomach (Levinthal & Strick, 2020) and diaphragm (Gandevia & Rothwell, 1987; Helou & Dum, 2023; Ramsay et al., 1993). Stimulation of the motor and premotor cortices alters heart rate (Mauck & Hockman, 1967). The location of these representations with respect to the classical homunculus is not yet known, although in humans they could contribute to the recently uncovered inter-effector regions in M1 (Gordon et al., 2023). Previous work demonstrated that cortical neurons in rat motor cortex influence specifically sympathic output to the stomach, and suggested colocalization of skeletomotor and sympathic function within the same cortical region might facilitate coordination of the two functions (Levinthal & Strick, 2020).

Different lines of evidence point toward a link between the gastric rhythm, dopamine and the motor system. In mice, stimulation of gastric vagal afferents stimulates dopamine release in the nigro-striatal pathway (Han et al., 2018). Beyond a modulation of food-seeking behaviour (Fernandes et al., 2020; Han et al., 2018), dopamine modulation of the nigro-striatal pathway might affect motor behaviour via the basal ganglia motor loop. In humans, gastro-intestinal symptoms are commonly reported in Parkinson's disease, with irregularities in the electrogastrogram (Araki et al., 2021). Interestingly, deep brain stimulation of the sub-thalamic nucleus alleviates both motor and gastric symptoms (Krygowska-Wajs et al., 2016). Collectively, those findings suggest that dopamine in the nigro-striatal system might be involved in the gastric-motor coupling we observe here – in other words, the coupling itself could begin outside primary motor cortex, but be revealed by TMS stimulation of the primary motor cortex. At the opposite end of the spectrum, mechanisms might be very local. For instance, the cardiac rhythm might be transduced directly in the motor cortex (Jammal Salameh et al., 2024; Kim et al., 2016), and exert a direct impact on local excitation/inhibition balance, in line with recent findings that cardiac effects on motor cortex are mediated by $GABA_A$ in humans (Paci et al., 2024).

Lastly, the observed effects might either partially or fully occur at more peripheral levels, as the motor evoked potential reflects a compound measure of cortical, spinal and muscle excitability (Spampinato et al., 2023). The cardiac rhythm has previously been shown to modulate alpha motoneuron discharges in cats (Ford & Kirkwood, 2018), and muscle activity in humans (Birznieks et al., 2012). However Transcranial Evoked Potentials, i.e. the cortical response to TMS pulse measured with EEG that reflect cortical excitability only (Hernandez-Pavon et al., 2023), differ in amplitude between cardiac systole and diastole (Al et al., 2023). Therefore, at least the observed modulation of MEPs by the cardiac cycle in the current experiment might represent a mixture of alterations in both cortical and spinal excitability.

4.3 Distinct dimensions and modalities in interoception

The fact that different visceral rhythms are independently coupled with corticospinal excitability echoes recent calls to consider organ-specificity in interoception (Desmedt et al., 2023; Engelen et al., 2023). Interoception has already been subdivided in distinct dimensions, which include, among others, self-reported interoception as measured through questionnaires, the accuracy by which one can perceive interoceptive signals, or neural representations of interoceptive signals (Suksasilp & Garfinkel, 2022). So far, the idea that each organ might be sensed differently within the different dimensions of interoception has been investigated on the level of interoceptive accuracy. Here, cardiac, respiratory, and gastric interoceptive accuracy seem independent from one another (Ferentzi, Bogdány, et al., 2018; Garfinkel et al., 2016; Van Den Houte et al., 2021; Werner et al., 2009). Our results further underscore the importance of treating self-reports as a distinct dimension of interoception, as here they were unrelated to the neural dimension of interoception. Previous lack of correlations between self-reports and interoceptive accuracy in the cardiac domain (Calì et al., 2015; Critchley et al., 2004; Ferentzi, Drew, et al., 2018) may have been partially driven by questionnaires conflating multiple viscera and fundamentally tapping into different constructs (Desmedt et al., 2022). To partly overcome this limitation, here correlations were calculated between organ-specific self-reports (Vlemincx et al., 2023) with their respective organ-motor coupling score. Despite this, we still found no significant correlations between self-reported and neural interoceptive measures. This is in line with previous evidence showing that, even when directly probed, participants reported no awareness between coupling of motor actions and respiratory phase (Park et al., 2020). Neural and self-reported questionnaire measures of interoception thus reflect distinct interoceptive dimensions, within which the different organs represent separate modalities.

4.4 Functional relevance of viscera-motor coupling

Signals from the viscera have been linked to actions in the contexts of exploration, food seeking behaviour, and fight/flight responses. For example, in rodents respiratory phase is locked to onsets of whisker, nose, and head movements (Kleinfeld et al., 2023; Kurnikova et al., 2017), which forms a strategic behavioural exploration state (Findley et al., 2021). Gastric vagally mediated dopamine neuron activity plays an essential role in post-ingestive dependent food seeking (Fernandes et al., 2020). In humans, this resembles findings of environmental sampling locked to the cardiac phase (Galvez-Pol et al., 2020, 2022) and locking of respiratory cycle to stimulus onsets (Perl et al., 2019). Visceral signals have additionally been associated to defensive actions in mice. Respiratory entrainment of the olfactory bulb is necessary to initiate freezing behaviour (Bagur et al., 2018), and induced tachycardia leads to anxiety like behaviour in risky situations (Hsueh et al., 2023). The link between visceral rhythms and the motor system thus seems to support certain behavioural states, however the functional relevance of idiosyncratic coupling profiles is more speculative and thus far not explored. The above-mentioned research suggests a certain degree of state dependence of viscera-brain coupling (e.g. when exploring the environment), something which was not tested in the current experiment. The levels of viscera-motor coupling as well as the independence of the viscera might thus be dynamic and depend on task demand.

In addition to this, interoceptive profiles might be linked to mental health and psychiatric disorders. Some affective disorders have already been linked to disrupted interoception in one bodily axis (Khalsa et al., 2018; Nord & Garfinkel, 2022; Saltafossi et al., 2024), for example recent findings relating increased gastric-brain coupling to anxiety (Banellis et al., 2024). Further specification however might find that either specific disorders or transdiagnostic markers are characterized by distinct combinations of hypo- and hyper-coupling between the brain and the different viscera. Lastly, interoceptive profiles might be linked to neurological disorders. While many patients with Parkinson's disease suffer from gastric motility issues (Araki et al., 2021), Alzheimer's disease is associated with olfactory deficits (Murphy, 2019). Taken together, our results show the need for future research to map interoception across dimensions and bodily axes to better understand individual differences in health and disease (Candia-Rivera et al., 2024; Kluger et al., 2024; Suksasilp & Garfinkel, 2022).

4.5 Conclusion

The coupling between motor excitability and the gastric, respiratory and cardiac rhythms can be measured by probing the cortico-spinal excitability of the hand. All three rhythms impact the motor control of the hand, but independently. These findings have important consequences for how interoception is conceptualized: distinct mechanism underly coupling between the

visceral rhythms and the motor system. Going forward, multi-organ recordings combined with neuroimaging are needed to reveal the functional relevance of interoceptive profiles, with potential implications in the fields of interoception, psychiatry, and neurology.

Acknowledgements

The authors thank Camille Straboni for her help in developing the respiration preprocessing pipeline. This work was funded by Agence Nationale pour la Recherche (ANR- 17-EURE-0017, ANR-10- IDEX-0001-02, ANR- 21-CE37-0031). CTB is supported by a senior fellowship of the Canadian Institute For Advanced Research (CI-FAR) program in Brain, Mind and Consciousness. A CC-BY public copyright license has been applied by the authors to the present document and will be applied to all subsequent versions up to the Author Accepted Manuscript arising from this submission, in accordance with the grant's open access conditions.

Data & code availability

The custom code and preprocessed data used for the analyses reported in this article will be made available online through an open repository upon journal publication. Due to data protection regulations in the EU, individual anatomical MRI data cannot be made available online.

Credit authorship contribution statement

TE: conceptualization, methodology, formal analysis, investigation, data curation, writing original draft & editing, funding acquisition. TS & ATS: conceptualization, resources & writing – review & editing. CTB: conceptualization, methodology, formal analysis, writing original draft & editing, funding acquisition, supervision, project administration.

References

Al, E., Stephani, T., Engelhardt, M., Haegens, S., Villringer, A., & Nikulin, V. V. (2023). Cardiac activity impacts cortical motor excitability. *PLOS Biology*, *21*(11), e3002393. https://doi.org/10.1371/journal.pbio.3002393

Araki, N., Yamanaka, Y., Poudel, A., Fujinuma, Y., Katagiri, A., Kuwabara, S., & Asahina, M. (2021). Electrogastrography for diagnosis of early-stage Parkinson's disease. *Parkinsonism & Related Disorders*, *86*, 61–66. https://doi.org/10.1016/j.parkreldis.2021.03.016

Bagur, S., Lefort, J. M., Lacroix, M. M., de Lavilléon, G., Herry, C., Billand, C., Geoffroy, H., & Benchenane, K. (2018). *Dissociation of fear initiation and maintenance by breathing-driven prefrontal oscillations* [Preprint]. Neuroscience. https://doi.org/10.1101/468264

Banellis, L., Rebollo, I., Nikolova, N., & Allen, M. (2024). *Increased stomach-brain coupling indexes a dimensional signature of negative mental health symptoms*. https://doi.org/10.1101/2024.06.05.597517

Bestmann, S., & Krakauer, J. W. (2015). The uses and interpretations of the motor-evoked potential for understanding behaviour. *Experimental Brain Research*, *233*(3), 679–689. https://doi.org/10.1007/s00221-014-4183-7

Bianchini, E., Mancuso, M., Zampogna, A., Guerra, A., & Suppa, A. (2021). Cardiac cycle does not affect motor evoked potential variability: A real-time EKG-EMG study. *Brain Stimulation*, *14*(1), 170–172. https://doi.org/10.1016/j.brs.2020.12.009

Birznieks, I., Boonstra, T. W., & Macefield, V. G. (2012). Modulation of Human Muscle Spindle Discharge by Arterial Pulsations—Functional Effects and Consequences. *PLOS ONE*, *7*(4), e35091. https://doi.org/10.1371/journal.pone.0035091

Calì, G., Ambrosini, E., Picconi, L., Mehling, W., & Committeri, G. (2015). Investigating the relationship between interoceptive accuracy, interoceptive awareness, and emotional susceptibility. *Frontiers in Psychology*, *6*. https://doi.org/10.3389/fpsyg.2015.01202

Candia-Rivera, D., Engelen, T., Babo-Rebelo, M., & Salamone, P. C. (2024). Interoception, network physiology and the emergence of bodily self-awareness. *Neuroscience & Biobehavioral Reviews*, *165*, 105864. https://doi.org/10.1016/j.neubiorev.2024.105864

Cao, J., Lu, K.-H., Oleson, S. T., Phillips, R. J., Jaffey, D., Hendren, C. L., Powley, T. L., & Liu, Z. (2019). Gastric stimulation drives fast BOLD responses of neural origin. *NeuroImage*, *197*, 200–211. https://doi.org/10.1016/j.neuroimage.2019.04.064

Cao, J., Wang, X., Chen, J., Zhang, N., & Liu, Z. (2022). The vagus nerve mediates the stomach-brain coherence in rats. *NeuroImage*, *263*, 119628. https://doi.org/10.1016/j.neuroimage.2022.119628

Claudino, L., Hussain, S. J., Buch, E. R., & Cohen, L. G. (2018). *Offline coil position denoising enhances detection of TMS effects* (p. 256081). bioRxiv. https://doi.org/10.1101/256081

Critchley, H. D., Wiens, S., Rotshtein, P., Öhman, A., & Dolan, R. J. (2004). Neural systems supporting interoceptive awareness. *Nature Neuroscience*, *7*(2), 189–195. https://doi.org/10.1038/nn1176

Desmedt, O., Heeren, A., Corneille, O., & Luminet, O. (2022). What do measures of self-report interoception measure? Insights from a systematic review, latent factor analysis, and network approach. *Biological Psychology*, *169*, 108289. https://doi.org/10.1016/j.biopsycho.2022.108289

Desmedt, O., Luminet, O., Maurage, P., & Corneille, O. (2023). Discrepancies in the Definition and Measurement of Human Interoception: A Comprehensive Discussion and Suggested Ways Forward. *Perspectives on Psychological Science*, 17456916231191537. https://doi.org/10.1177/17456916231191537

Engelen, T., Solcà, M., & Tallon-Baudry, C. (2023). Interoceptive rhythms in the brain. *Nature Neuroscience*, *26*(10), 1670–1684. https://doi.org/10.1038/s41593-023-01425-1

Faul, F., Erdfelder, E., Lang, A.-G., & Buchner, A. (2007). G*Power 3: A flexible statistical power analysis program for the social, behavioral, and biomedical sciences. *Behavior Research Methods*, *39*(2), 175–191. https://doi.org/10.3758/BF03193146

Ferentzi, E., Bogdány, T., Szabolcs, Z., Csala, B., Horváth, Á., & Köteles, F. (2018). Multichannel Investigation of Interoception: Sensitivity Is Not a Generalizable Feature. *Frontiers in Human Neuroscience*, *12*. https://doi.org/10.3389/fnhum.2018.00223

Ferentzi, E., Drew, R., Tihanyi, B. T., & Köteles, F. (2018). Interoceptive accuracy and body awareness – Temporal and longitudinal associations in a non-clinical sample. *Physiology & Behavior*, *184*, 100–107. https://doi.org/10.1016/j.physbeh.2017.11.015

Fernandes, A. B., Silva, J. A. da, Almeida, J., Cui, G., Gerfen, C. R., Costa, R. M., & Oliveira-Maia, A. J. (2020). Postingestive Modulation of Food Seeking Depends on Vagus-Mediated Dopamine Neuron Activity. *Neuron*, *106*(5), 778-788.e6. https://doi.org/10.1016/j.neuron.2020.03.009

Filippi, M. M., Oliveri, M., Vernieri, F., Pasqualetti, P., & Rossini, P. M. (2000). Are autonomic signals influencing cortico-spinal motor excitability?: A study with transcranial magnetic stimulation. *Brain Research*, *881*(2), 159–164. https://doi.org/10.1016/S0006-8993(00)02837-7

Findley, T. M., Wyrick, D. G., Cramer, J. L., Brown, M. A., Holcomb, B., Attey, R., Yeh, D., Monasevitch, E., Nouboussi, N., Cullen, I., Songco, J. O., King, J. F., Ahmadian, Y., & Smear, M. C. (2021). Sniff-synchronized, gradient-guided olfactory search by freely moving mice. *eLife*, *10*, e58523. https://doi.org/10.7554/eLife.58523

Ford, T. W., & Kirkwood, P. A. (2018). Cardiac modulation of alpha motoneuron discharges. *Journal of Neurophysiology*, *119*(5), 1723–1730. https://doi.org/10.1152/jn.00025.2018

Galvez-Pol, A., McConnell, R., & Kilner, J. M. (2020). Active sampling in visual search is coupled to the cardiac cycle. *Cognition*, *196*, 104149. https://doi.org/10.1016/j.cognition.2019.104149

Galvez-Pol, A., Virdee, P., Villacampa, J., & Kilner, J. (2022). Active tactile discrimination is coupled with and modulated by the cardiac cycle. *eLife*, *11*, e78126. https://doi.org/10.7554/eLife.78126

Gandevia, S. C., & Rothwell, J. C. (1987). Activation of the human diaphragm from the motor cortex. *The Journal of Physiology*, *384*(1), 109–118. https://doi.org/10.1113/jphysiol.1987.sp016445

Garfinkel, S. N., Manassei, M. F., Hamilton-Fletcher, G., In den Bosch, Y., Critchley, H. D., & Engels, M. (2016). Interoceptive dimensions across cardiac and respiratory axes. *Philosophical Transactions of the Royal Society B: Biological Sciences*, *371*(1708), 20160014. https://doi.org/10.1098/rstb.2016.0014

González, J., Cavelli, M., Mondino, A., Castro-Zaballa, S., Brankačk, J., Draguhn, A., Torterolo, P., & Tort, A. B. L. (2023). Breathing modulates gamma synchronization across species. *Pflugers Archiv: European Journal of Physiology*, *475*(1), 49–63. https://doi.org/10.1007/s00424-022-02753-0

Gonzalez, J., Torterolo, P., & Tort, A. B. (2023). Mechanisms and functions of respiration-driven gamma oscillations in the primary olfactory cortex. *eLife*, *12*, e83044. https://doi.org/10.7554/eLife.83044

Gordon, E. M., Chauvin, R. J., Van, A. N., Rajesh, A., Nielsen, A., Newbold, D. J., Lynch, C. J., Seider, N. A., Krimmel, S. R., Scheidter, K. M., Monk, J., Miller, R. L., Metoki, A., Montez, D. F., Zheng, A., Elbau, I., Madison, T., Nishino, T., Myers, M. J., … Dosenbach, N. U. F. (2023). A somato-cognitive action network alternates with effector regions in motor cortex. *Nature*, *617*(7960), 351–359. https://doi.org/10.1038/s41586-023-05964-2

Grosmaitre, X., Santarelli, L. C., Tan, J., Luo, M., & Ma, M. (2007). Dual functions of mammalian olfactory sensory neurons as odor detectors and mechanical sensors. *Nature Neuroscience*, *10*(3), 348–354. https://doi.org/10.1038/nn1856

Han, W., Tellez, L. A., Perkins, M. H., Perez, I. O., Qu, T., Ferreira, J., Ferreira, T. L., Quinn, D., Liu, Z.-W., Gao, X.-B., Kaelberer, M. M., Bohórquez, D. V., Shammah-Lagnado, S. J., Lartigue, G. de, & Araujo, I. E. de. (2018). A Neural Circuit for Gut-Induced Reward. *Cell*, *175*(3), 665-678.e23. https://doi.org/10.1016/j.cell.2018.08.049

Helou, L. B., & Dum, R. P. (2023). Volitional inspiration is mediated by two independent output channels in the primary motor cortex. *Journal of Comparative Neurology*, *531*(17), 1796–1811. https://doi.org/10.1002/cne.25540

Hernandez-Pavon, J. C., Veniero, D., Bergmann, T. O., Belardinelli, P., Bortoletto, M., Casarotto, S., Casula, E. P., Farzan, F., Fecchio, M., Julkunen, P., Kallioniemi, E., Lioumis, P., Metsomaa, J., Miniussi, C., Mutanen, T. P., Rocchi, L., Rogasch, N. C., Shafi, M. M., Siebner, H. R., … Ilmoniemi, R. J. (2023). TMS combined with EEG: Recommendations and open issues for data collection and analysis. *Brain Stimulation: Basic, Translational, and Clinical Research in Neuromodulation*, *16*(2), 567–593. https://doi.org/10.1016/j.brs.2023.02.009

Hsueh, B., Chen, R., Jo, Y., Tang, D., Raffiee, M., Kim, Y. S., Inoue, M., Randles, S., Ramakrishnan, C., Patel, S., Kim, D. K., Liu, T. X., Kim, S. H., Tan, L., Mortazavi, L., Cordero, A., Shi, J., Zhao, M., Ho, T. T., … Deisseroth, K. (2023). Cardiogenic control of affective behavioural state. *Nature*, *615*(7951), 292–299. https://doi.org/10.1038/s41586-023-05748-8

Hülsemann, M. J., Naumann, E., & Rasch, B. (2019). Quantification of Phase-Amplitude Coupling in Neuronal Oscillations: Comparison of Phase-Locking Value, Mean Vector Length, Modulation Index, and Generalized-Linear-Modeling-Cross-Frequency-Coupling. *Frontiers in Neuroscience*, *13*. https://doi.org/10.3389/fnins.2019.00573

Jammal Salameh, L., Bitzenhofer, S. H., Hanganu-Opatz, I. L., Dutschmann, M., & Egger, V. (2024). Blood pressure pulsations modulate central neuronal activity via mechanosensitive ion channels. *Science*, *383*(6682), eadk8511. https://doi.org/10.1126/science.adk8511

Johannknecht, M., & Kayser, C. (2022). The influence of the respiratory cycle on reaction times in sensory-cognitive paradigms. *Scientific Reports*, *12*(1), 2586. https://doi.org/10.1038/s41598-022-06364-8

Khalsa, S. S., Adolphs, R., Cameron, O. G., Critchley, H. D., Davenport, P. W., Feinstein, J. S., Feusner, J. D., Garfinkel, S. N., Lane, R. D., Mehling, W. E., Meuret, A. E., Nemeroff, C. B., Oppenheimer, S., Petzschner, F. H., Pollatos, O., Rhudy, J. L., Schramm, L. P., Simmons, W. K., Stein, M. B., … Zucker, N. (2018). Interoception and Mental Health: A Roadmap. *Biological Psychiatry: Cognitive Neuroscience and Neuroimaging*, *3*(6), 501–513. https://doi.org/10.1016/j.bpsc.2017.12.004

Kim, K. J., Diaz, J. R., Iddings, J. A., & Filosa, J. A. (2016). Vasculo-Neuronal Coupling: Retrograde Vascular Communication to Brain Neurons. *Journal of Neuroscience*, *36*(50), 12624–12639. https://doi.org/10.1523/JNEUROSCI.1300-16.2016

Kleinfeld, D., Deschênes, M., Economo, M. N., Elbaz, M., Golomb, D., Liao, S.-M., O'Connor, D. H., & Wang, F. (2023). Low- and high-level coordination of orofacial motor actions. *Current Opinion in Neurobiology*, *83*, 102784. https://doi.org/10.1016/j.conb.2023.102784

Kluger, D. S., Allen, M. G., & Gross, J. (2024). Brain–body states embody complex temporal dynamics. *Trends in Cognitive Sciences*, *0*(0). https://doi.org/10.1016/j.tics.2024.05.003

Kluger, D. S., & Gross, J. (2020). Depth and phase of respiration modulate cortico-muscular communication. *NeuroImage*, *222*, 117272. https://doi.org/10.1016/j.neuroimage.2020.117272

Kluger, D. S., & Gross, J. (2021). Respiration modulates oscillatory neural network activity at rest. *PLOS Biology*, *19*(11), e3001457. https://doi.org/10.1371/journal.pbio.3001457

Konttinen, N., Mets, T., Lyytinen, H., & Paananen, M. (2003). Timing of Triggering in Relation to the Cardiac Cycle in Nonelite Rifle Shooters. *Research Quarterly for Exercise and Sport*. https://www.tandfonline.com/doi/abs/10.1080/02701367.2003.10609110

Kramer, M. A., & Eden, U. T. (2013). Assessment of cross-frequency coupling with confidence using generalized linear models. *Journal of Neuroscience Methods*, *220*(1), 64–74. https://doi.org/10.1016/j.jneumeth.2013.08.006

Krygowska-Wajs, A., Furgala, A., Gorecka-Mazur, A., Pietraszko, W., Thor, P., Potasz-Kulikowska, K., & Moskala, M. (2016). The effect of subthalamic deep brain stimulation on gastric motility in Parkinson's disease. *Parkinsonism & Related Disorders*, *26*, 35–40. https://doi.org/10.1016/j.parkreldis.2016.02.010

Kunzendorf, S., Klotzsche, F., Akbal, M., Villringer, A., Ohl, S., & Gaebler, M. (2019). Active information sampling varies across the cardiac cycle. *Psychophysiology*, *56*(5), e13322. https://doi.org/10.1111/psyp.13322

Kurnikova, A., Moore, J. D., Liao, S.-M., Deschênes, M., & Kleinfeld, D. (2017). Coordination of Orofacial Motor Actions into Exploratory Behavior by Rat. *Current Biology*, *27*(5), 688–696. https://doi.org/10.1016/j.cub.2017.01.013

Levinthal, D. J., & Strick, P. L. (2020). Multiple areas of the cerebral cortex influence the stomach. *Proceedings of the National Academy of Sciences*, *117*(23), 13078–13083. https://doi.org/10.1073/pnas.2002737117

Li, S., & Rymer, W. Z. (2011). Voluntary Breathing Influences Corticospinal Excitability of Nonrespiratory Finger Muscles. *Journal of Neurophysiology*, *105*(2), 512–521. https://doi.org/10.1152/jn.00946.2010

Liang, F., Paulo, R., Molina, G., Clyde, M. A., & Berger, J. O. (2008). Mixtures of g Priors for Bayesian Variable Selection. *Journal of the American Statistical Association*, *103*(481), 410–423. https://doi.org/10.1198/016214507000001337

Mauck, H. P., & Hockman, C. H. (1967). Central nervous system mechanisms mediating cardiac rate and rhythm. *American Heart Journal*, *74*(1), 96–109. https://doi.org/10.1016/0002-8703(67)90047-6

Mehling, W. E., Acree, M., Stewart, A., Silas, J., & Jones, A. (2018). The Multidimensional Assessment of Interoceptive Awareness, Version 2 (MAIA-2). *PLOS ONE*, *13*(12), e0208034. https://doi.org/10.1371/journal.pone.0208034

Murphy, C. (2019). Olfactory and other sensory impairments in Alzheimer disease. *Nature Reviews Neurology*, *15*(1), 11–24. https://doi.org/10.1038/s41582-018-0097-5

Nord, C. L., & Garfinkel, S. N. (2022). Interoceptive pathways to understand and treat mental health conditions. *Trends in Cognitive Sciences*, *26*(6), 499–513. https://doi.org/10.1016/j.tics.2022.03.004

Ohl, S., Wohltat, C., Kliegl, R., Pollatos, O., & Engbert, R. (2016). Microsaccades Are Coupled to Heartbeat. *Journal of Neuroscience*, *36*(4), 1237–1241. https://doi.org/10.1523/JNEUROSCI.2211-15.2016

Oostenveld, R., Fries, P., Maris, E., & Schoffelen, J.-M. (2011). FieldTrip: Open Source Software for Advanced Analysis of MEG, EEG, and Invasive Electrophysiological Data. *Computational Intelligence and Neuroscience*, *2011*, 1–9. https://doi.org/10.1155/2011/156869

Otsuru, N., Miyaguchi, S., Kojima, S., Yamashiro, K., Sato, D., Yokota, H., Saito, K., Inukai, Y., & Onishi, H. (2020). Timing of Modulation of Corticospinal Excitability by Heartbeat Differs with Interoceptive Accuracy. *Neuroscience*, *433*, 156–162. https://doi.org/10.1016/j.neuroscience.2020.03.014

Paci, M., Cardellicchio, P., Di Luzio, P., Perrucci, M. G., Ferri, F., & Costantini, M. (2024). When the heart inhibits the brain: Cardiac phases modulate short-interval intracortical inhibition. *iScience*, *27*(3), 109140. https://doi.org/10.1016/j.isci.2024.109140

Palser, E. R., Glass, J., Fotopoulou, A., & Kilner, J. M. (2021). Relationship between cardiac cycle and the timing of actions during action execution and observation. *Cognition*, *217*, 104907. https://doi.org/10.1016/j.cognition.2021.104907

Park, H.-D., Barnoud, C., Trang, H., Kannape, O. A., Schaller, K., & Blanke, O. (2020). Breathing is coupled with voluntary action and the cortical readiness potential. *Nature Communications*, *11*(1), 289. https://doi.org/10.1038/s41467-019-13967-9

Park, H.-D., & Blanke, O. (2019). Heartbeat-evoked cortical responses: Underlying mechanisms, functional roles, and methodological considerations. *Neuroimage*, *197*, 502–511.

Perl, O., Ravia, A., Rubinson, M., Eisen, A., Soroka, T., Mor, N., Secundo, L., & Sobel, N. (2019). Human non-olfactory cognition phase-locked with inhalation. *Nature Human Behaviour*, *3*(5), 501–512. https://doi.org/10.1038/s41562-019-0556-z

Rae, C. L., Botan, V. E., Gould van Praag, C. D., Herman, A. M., Nyyssönen, J. A. K., Watson, D. R., Duka, T., Garfinkel, S. N., & Critchley, H. D. (2018). Response inhibition on the stop signal task improves during cardiac contraction. *Scientific Reports*, *8*(1), 9136. https://doi.org/10.1038/s41598-018-27513-y

Ramsay, S. C., Adams, L., Murphy, K., Corfield, D. R., Grootoonk, S., Bailey, D. L., Frackowiak, R. S., & Guz, A. (1993). Regional cerebral blood flow during volitional expiration in man: A comparison with volitional inspiration. *The Journal of Physiology*, *461*(1), 85–101. https://doi.org/10.1113/jphysiol.1993.sp019503

Rebollo, I., Devauchelle, A.-D., Béranger, B., & Tallon-Baudry, C. (2018). Stomach-brain synchrony reveals a novel, delayed-connectivity resting-state network in humans. *eLife*, *7*, e33321. https://doi.org/10.7554/eLife.33321

Rebollo, I., & Tallon-Baudry, C. (2022). The sensory and motor components of the cortical hierarchy are coupled to the rhythm of the stomach during rest. *Journal of Neuroscience*, *42*(11), 2205–2220. https://doi.org/10.1523/JNEUROSCI.1285-21.2021

Richter, C. G., Babo-Rebelo, M., Schwartz, D., & Tallon-Baudry, C. (2017). Phase-amplitude coupling at the organism level: The amplitude of spontaneous alpha rhythm fluctuations varies with the phase of the infra-slow gastric basal rhythm. *NeuroImage*, *146*, 951–958. https://doi.org/10.1016/j.neuroimage.2016.08.043

Saltafossi, M., Heck, D., Kluger, D., & Varga, S. (2024). *Common Threads: Altered Interoceptive Processes as Transdiagnostic Mechanisms Across Affective and Anxiety disorders*. OSF. https://doi.org/10.31234/osf.io/3d745

Schulz, A., Schilling, T. M., Vögele, C., Larra, M. F., & Schächinger, H. (2016). Respiratory modulation of startle eye blink: A new approach to assess afferent signals from the respiratory system. *Philosophical Transactions of the Royal Society B: Biological Sciences*, *371*(1708), 20160019. https://doi.org/10.1098/rstb.2016.0019

Shirakawa, K., Yunoki, T., Afroundeh, R., Lian, C.-S., Matsuura, R., Ohtsuka, Y., & Yano, T. (2015). Voluntary breathing increases corticospinal excitability of lower limb muscle during isometric contraction. *Respiratory Physiology & Neurobiology*, *217*, 40–45. https://doi.org/10.1016/j.resp.2015.07.003

Spampinato, D. A., Ibanez, J., Rocchi, L., & Rothwell, J. (2023). Motor potentials evoked by transcranial magnetic stimulation: Interpreting a simple measure of a complex system. *The Journal of Physiology*, *601*(14), 2827–2851. https://doi.org/10.1113/JP281885

Suksasilp, C., & Garfinkel, S. N. (2022). Towards a comprehensive assessment of interoception in a multi-dimensional framework. *Biological Psychology*, *168*, 108262. https://doi.org/10.1016/j.biopsycho.2022.108262

Tort, A. B. L., Komorowski, R., Eichenbaum, H., & Kopell, N. (2010). Measuring Phase-Amplitude Coupling Between Neuronal Oscillations of Different Frequencies. *Journal of Neurophysiology*, *104*(2), 1195–1210. https://doi.org/10.1152/jn.00106.2010

Van Den Houte, M., Vlemincx, E., Franssen, M., Van Diest, I., Van Oudenhove, L., & Luminet, O. (2021). The respiratory occlusion discrimination task: A new paradigm to measure respiratory interoceptive accuracy. *Psychophysiology*, *58*(4), e13760. https://doi.org/10.1111/psyp.13760

Vázquez-Seisdedos, C. R., Neto, J. E., Marañón Reyes, E. J., Klautau, A., & Limão de Oliveira, R. C. (2011). New approach for T-wave end detection on electrocardiogram: Performance in noisy conditions. *BioMedical Engineering OnLine*, *10*(1), 77. https://doi.org/10.1186/1475-925X-10-77

Vlemincx, E., Walentynowicz, M., Zamariola, G., Van Oudenhove, L., & Luminet, O. (2023). A novel self-report scale of interoception: The three-domain interoceptive sensations questionnaire (THISQ). *Psychology & Health*, *38*(9), 1234–1253. https://doi.org/10.1080/08870446.2021.2009479

Werner, N. S., Duschek, S., Mattern, M., & Schandry, R. (2009). The Relationship Between Pain Perception and Interoception. *Journal of Psychophysiology*, *23*(1), 35–42. https://doi.org/10.1027/0269-8803.23.1.35

Wolpert, N., Rebollo, I., & Tallon-Baudry, C. (2020). Electrogastrography for psychophysiological research: Practical considerations, analysis pipeline, and normative data in a large sample. *Psychophysiology*, *57*(9). https://doi.org/10.1111/psyp.13599

Zhuang, L., Zhang, B., Qin, Z., & Wang, P. (2019). Nasal Respiration is Necessary for the Generation of γ Oscillation in the Olfactory Bulb. *Neuroscience*, *398*, 218–230. https://doi.org/10.1016/j.neuroscience.2018.12.011